Available online at www.sciencedirect.com
ScienceDirect
Journal of Organometallic Chemistry 692 (2007) 3823–3834
Journal of Organometallic Chemistry
www.elsevier.com/locate/jorganchem

Rare earth metal alkyl complexes bearing *N*,*O*,*P* multidentate ligands: Synthesis, characterization and catalysis on the ring-opening polymerization of L-lactide

Wei Miao [a,c], Shihui Li [a,c], Dongmei Cui [a,b,*], Baotong Huang [a]

[a] *State Key Laboratory of Polymer Physics and Chemistry, Changchun Institute of Applied Chemistry, Chinese Academy of Sciences, Changchun 130022, China*

[b] *Ministry-of-Education Key Laboratory for the Synthesis and Application of Organic Functional Molecules, Hubei University, 430062, China*

[c] *Graduate School of the Chinese Academy of Sciences, Beijing 100039, China*

Received 20 April 2007; received in revised form 19 May 2007; accepted 21 May 2007
Available online 2 June 2007

Abstract

Alkane elimination reactions of rare earth metal tris(alkyl)s, $Ln(CH_2SiMe_3)_3(THF)_2$ (Ln = Y, Lu) with the multidentate ligands HL^{1-4}, afforded a series of new rare earth metal complexes. Yttrium complex **1** supported by flexible amino-imino phenoxide ligand HL^1 was isolated as homoleptic product. In the reaction of rigid phosphino-imino phenoxide ligand HL^2 with equimolar $Ln(CH_2SiMe_3)_3(THF)_2$, HL^2 was deprotonated by the metal alkyl and its imino C=N group was reduced to C–N by intramolecular alkylation, generating THF-solvated mono-alkyl complexes (**2a**: Ln = Y; **2b**: Ln = Lu). The di-ligand chelated yttrium complex **3** without alkyl moiety was isolated when the molar ratio of HL^2 to $Y(CH_2SiMe_3)_3(THF)_2$ increased to 2:1. Reaction of steric phosphino β-ketoiminato ligand HL^3 with equimolar $Ln(CH_2SiMe_3)_3(THF)_2$ afforded di-ligated mono-alkyl complexes (**4a**: Ln = Y; **4b**: Ln = Lu) without occurrence of intramolecular alkylation or formation of homoleptic product. Treatment of tetradentate methoxy-amino phenol HL^4 with $Y(CH_2SiMe_3)_3(THF)_2$ afforded a monomeric yttrium bis-alkyl complex of THF-free. The resultant complexes were characterized by IR, NMR spectrum and X-ray diffraction analyses. All alkyl complexes exhibited high activity toward the ring-opening polymerization of L-lactide to give isotactic polylactide with controllable molecular weight and narrow to moderate polydispersity.

Keywords: Rare earth metal; Alkyl complex; Multidentate; Lactide

1. Introduction

There is a growing interest in the past decades in the investigation of rare earth metal alkyl complexes that have shown tremendous catalytic activities toward olefin polymerization [1], highly regio- or stereo-selective polymerizations of conjugated monomers [2] and polar monomers [3]. Many ancillary ligands have been utilized to stabilize metal alkyls. The extensively developed family is cyclopentadienyl (Cp) and its derivatives [4]. Recently, research efforts have been directed towards non-Cp ligands by virtue of their exceptional and tunable steric and electronic features required for compensating coordinative unsaturation of metal centers [5–9]. However, rare earth metal alkyl, especially bis(alkyl) complexes supported by non-Cp ligands usually encounter salt addition, dimerization or ligand redistribution due to the highly active and relatively less steric characters of bis(alkyl) species. Thus, multidentate ligands have attracted more and more interests, which can provide proper sterics and electronics for the metal center to prevent the side-reactions mentioned above via varying the size and electron donor of the substituents.

* Corresponding author. Address: State Key Laboratory of Polymer Physics and Chemistry, Changchun Institute of Applied Chemistry, Chinese Academy of Sciences, Changchun 130022, China. Tel.: +86 431 85262773; fax: +86 431 85263773.
E-mail address: dmcui@ciac.jl.cn (D. Cui).

0022-328X/$ - see front matter © 2007 Elsevier B.V. All rights reserved.
doi:10.1016/j.jorganchem.2007.05.032

For example, tridentate phenoxytriamine [10], multidentate bis(oxazolinate)s [11] and tetradentate triazacyclononane-amide [12] have been reported to support rare earth metal amido or alkyl species.

Here, we wish to present the synthesis of a series of rare earth metal alkyl complexes supported by multidentate phenol with phosphino, amino or methoxy-amino functionalities and phosphino β-ketoimine auxiliaries. The dependence of molecular structures of the resultant complexes and their catalytic behavior towards the ring-opening polymerization (ROP) of L-lactide on the ligand framework will also be discussed.

2. Results and discussion

2.1. Syntheses and characterization of complexes

2.1.1. Synthesis and characterization of complex *1*

The protonolysis reaction of $Y(CH_2SiMe_3)_3(THF)_2$ with *N*,*N*,*O* tridentate ligand HL^1 was carried out in hexane at room temperature overnight to afford yellow solids, which was not the expected bis(alkyl) product but a tri-ligated complex $(L^1)_3Y$ (**1**) (Scheme 1). The ^1H NMR and ^{13}C NMR spectra were indicative to define the formation of complex **1** by the loss of the signal for phenol proton around δ 13.76. The molecular structure was further confirmed by X-ray diffraction to be seven-coordinate (Fig. 1). The yttrium atom bonded to three ligands, adopting distorted pentagonal bipyramidal geometry. The imino nitrogen N(1) and phenoxy oxygen O(2) were axial, while the phenoxy oxygen atoms O(1) and O(3), imino nitrogen atoms N(2) and N(3) and the amino nitrogen N(6) occupied the equatorial positions. No coordinated alkyl or THF moiety was observed. Two of the three ligands bonded to the yttrium ion in *N*,*O*-bidentate modes with the amino group hanging away from the metal center, whereas for the third ligand the amino nitrogen combined with the imino nitrogen and the phenoxy oxygen coordinated to the yttrium ion in *N*,*N*,*O*-tridentate mode. Thus the bite angles of O(1)–Y(1)–N(1) (74.49(18))°, O(2)–Y(1)–N(2) (74.78(18))° and O(3)–Y(1)–N(3) (72.20(18))° were different. This was in agreement with the NMR spectrum analysis. The methyl protons of NMe_2 group in complex **1** exhibited a broad resonance at δ 2.15 ppm, which was different from the singlet signal at δ 2.30 ppm in the free ligand. The bond distances between yttrium and the chelated nitrogen atoms Y(1)–N(1) (2.531(6) Å), Y(1)–N(2) (2.476(6) Å) and Y(1)–N(3) (2.509(6) Å) were close, which were shorter than that between yttrium and the pendent amino nitrogen atom Y(1)–N(6) (2.714(6) Å) (Table 1). The bond distances of N(1)–C(15) (1.276(9) Å), N(2)–C(34) (1.290(9) Å) and N(3)–C(53) (1.276(9) Å) were comparable to the established values observed for C=N double bond (1.294–1.312 Å) [13,14].

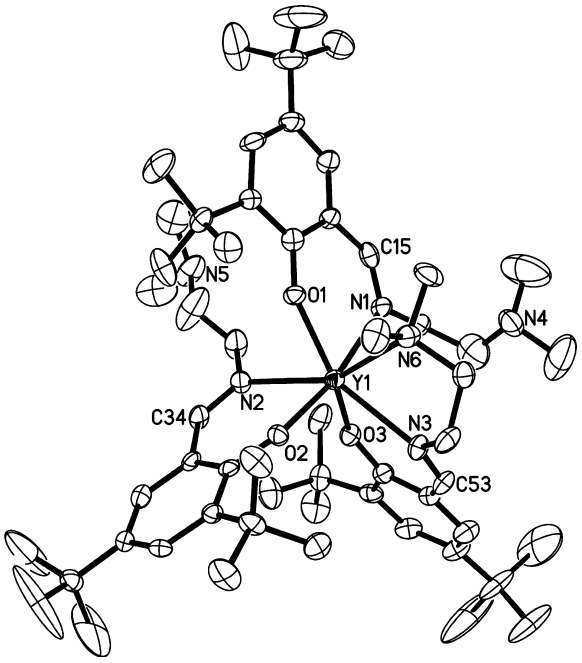

Fig. 1. X-ray structure of **1** with 35% probability of thermal ellipsoids, hydrogen atoms are omitted for clarity.

2.1.2. Syntheses and characterization of complexes *2a*, *2b* and *3*

Switching from the flexible ligand HL^1 to the rigid and bulky ligand HL^2 was expected to inhibit the formation of the homoleptic complex. The reaction of HL^2 with

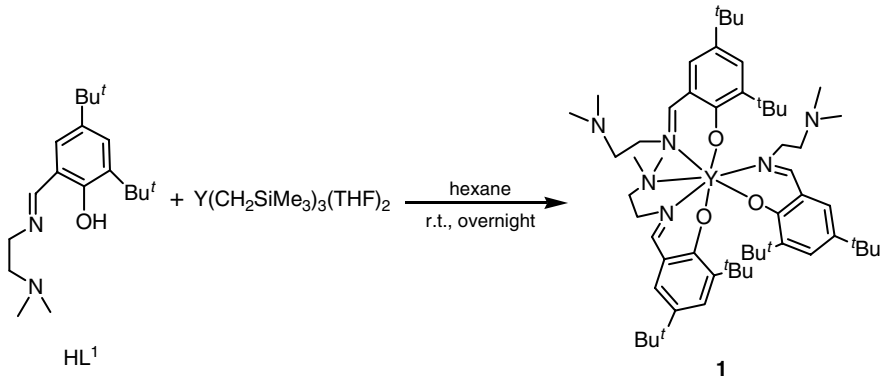

Scheme 1. Synthetic pathway for complex **1**.

Table 1
Selected bond lengths (Å) and angles (°) for complex **1**

Y(1)–N(2)	2.476(6)	Y(1)–O(2)	2.161(4)
Y(1)–N(3)	2.509(6)	Y(1)–O(1)	2.193(5)
Y(1)–N(1)	2.531(6)	Y(1)–O(3)	2.216(5)
Y(1)–N(6)	2.714(6)	N(3)–C(53)	1.276(9)
N(1)–C(15)	1.276(9)	N(2)–C(34)	1.290(9)
O(2)–Y(1)–N(1)	169.90(18)	O(2)–Y(1)–O(1)	97.12(17)
O(1)–Y(1)–N(1)	74.49(18)	O(2)–Y(1)–O(3)	102.16(18)
O(3)–Y(1)–N(1)	81.95(18)	O(1)–Y(1)–O(3)	141.52(18)
N(2)–Y(1)–N(1)	97.46(19)	O(2)–Y(1)–N(2)	74.78(18)
N(3)–Y(1)–N(1)	102.7(2)	O(1)–Y(1)–N(2)	76.54(19)
O(2)–Y(1)–N(6)	97.78(18)	O(3)–Y(1)–N(2)	76.89(19)
O(1)–Y(1)–N(6)	75.95(18)	O(2)–Y(1)–N(3)	87.33(18)
O(3)–Y(1)–N(6)	132.63(19)	O(1)–Y(1)–N(3)	142.23(19)
N(2)–Y(1)–N(6)	150.3(2)	O(3)–Y(1)–N(3)	72.20(19)
N(3)–Y(1)–N(6)	66.3(2)	N(2)–Y(1)–N(3)	139.9(2)
N(1)–Y(1)–N(6)	85.78(19)		

1 equiv. of $Y(CH_2SiMe_3)_3(THF)_2$ took place immediately upon addition to afford mono(alkyl) complex **2a**. Following the similar procedure, the lutetium analogue was obtained by treatment of HL^2 with 1 equiv. of $Lu(CH_2SiMe_3)_3(THF)_2$ (Scheme 2). The probable mechanistic pathway was described as Scheme 2. First, HL^2 protonated one metal alkyl species of $Ln(CH_2SiMe_3)_3(THF)_2$ with the release of tetramethylsilane to give a bis(alkyl) intermediate **A**. Unfortunately, **A** was not stable, the imino C=N group of which was then alkylated by intramolecular migration of the metal alkyl to generate $C(H)(CH_2SiMe_3)N$ species, leading to the formation of complex **2** eventually. The similar protonolysis accompanied by intramolecular alkyl migration was observed in the isolation of a pyrrolylaldiminato yttrium alkyl complex [15]. The methylene protons of $Y–CH_2SiMe_3$ in complex **2a** exhibiting a AB spin around δ −0.39 ppm shifted downfield compared to the singlet resonance around δ −0.6 ppm in the yttrium tris(alkyl)s. The intramolecular alkyl migration was confirmed by the formation of group $C(H)(CH_2SiMe_3)N$, which exhibited discrete doublet resonances at δ 1.21 and 2.08 ppm assigned to the diastereotopic methylene protons. The solid-state structure of complex **2a** was confirmed by X-ray diffraction analysis to be a monomer of six-coordinate with two solvated THF molecules. The geometry around the central metal was described as distorted tetragonal bipyramidal (Fig. 2). The bond distances between yttrium and THF oxygen atoms O(1) and O(3) were 2.355(2) Å and 2.397(2) Å, respectively, longer than the distance between yttrium and phenoxy oxygen Y–O(2) (2.119(2) Å) (Table 2). The bond length of C(19)–N (1.497(4) Å) was close to the normal C–N single bond (1.4904(17) Å) [13,14], indicating that the C=N bond of the ligand had been reduced to a single bond via intramolecular alkylation. The intramolecular alkylation has been found in *N*,*O* bidentate Salen titanium or zirconium bis(benzyl) complexes, which resulted in decomposition of the complexes and the loss of catalytic activity for ethylene polymerization [16].

The ^1H NMR spectrum and the X-ray analysis revealed that **2b** was an analogue of **2a** (Fig. 3). The slight difference between the structures of the two complexes was the bond angle of O(1)–Ln–O(3) being 174.83(7)° in **2a**, but much smaller (77.83(16)°) in **2b**, indicating the different arrangement of THF moieties (Table 2).

Treatment of $Y(CH_2SiMe_3)_3(THF)_2$ with 2 equiv. of HL^2 at room temperature for 12 h generated complex **3** in high yields (75%) via abstractions of metal alkyls (Scheme 2). The existence of the C=N bond was confirmed by the resonance around δ 7.90 ppm in ^1H NMR spectrum assigned to the imino proton of C*H*=N group. At the same

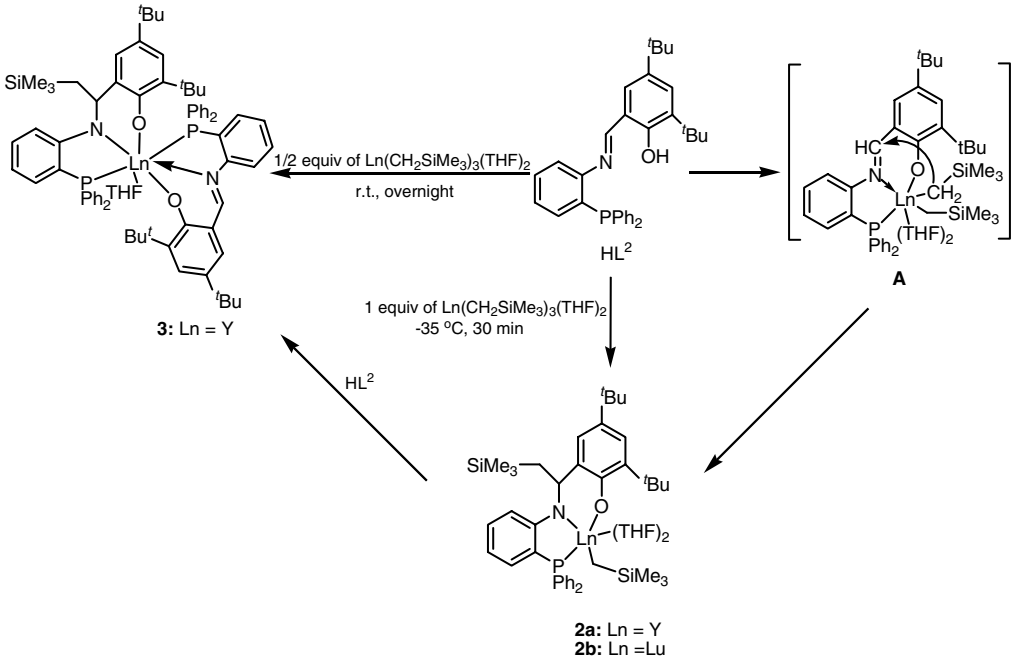

Scheme 2. Synthetic pathway for complexes **2a**, **2b** and **3**.

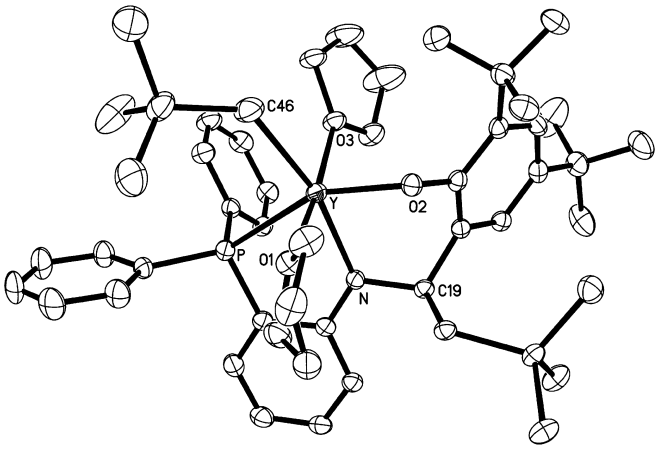

Fig. 2. X-ray structure of **2a** with 35% probability of thermal ellipsoids, hydrogen atoms are omitted for clarity.

Table 2
Selected bond lengths (Å) and angles (°) for complexes **2a** and **2b**

	2a	**2b**
Ln–O(2)	2.119(2)	2.064(4)
Ln–O(1)	2.355(2)	2.378(4)
Ln–O(3)	2.397(2)	2.434(4)
Ln–N	2.374(2)	2.254(5)
Ln–C(46)	2.451(4)	2.368(7)
Ln–P	2.9717(8)	2.9376(16)
N–C(18)	1.380(4)	1.369(7)
N–C(19)	1.497(4)	1.491(7)
O(2)–Ln–N	85.69(8)	88.15(16)
O(2)–Ln–C(46)	106.36(12)	103.5(2)
N–Ln–C(46)	166.74(11)	98.8(3)
O(2)–Ln–P	152.18(6)	153.74(12)
N–Ln–P	66.54(6)	69.04(12)
C(46)–Ln–P	101.44(11)	93.06(19)
O(1)–Ln–O(3)	174.83(7)	77.83(16)

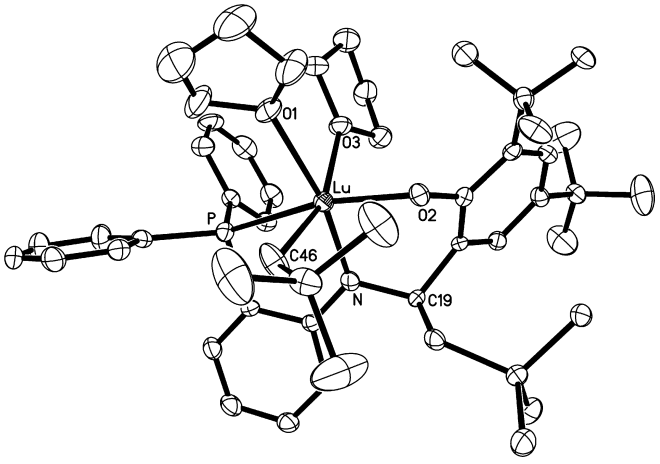

Fig. 3. X-ray structure of **2b** with 35% probability of thermal ellipsoids, hydrogen atoms are omitted for clarity.

time, the discrete doublet resonances around δ 1.16 and 1.99 ppm arising from the diastereotopic methylene protons of C(H)(CH_2SiMe_3)N group confirmed the intramolecular alkyl migration and the formation of C–N bond reduced from C=N. This might be a two-step process: firstly, reaction of $Y(CH_2SiMe_3)_3(THF)_2$ with equimolar HL^2 via intramolecular alkyl migration afforded **2a**, which reacted further with the excessive HL^2 via alkane elimination to generate **3**. If kept at room temperature for several days, **2a** would slowly disproportionate to **3**. Such disproportionation was also observed by Piers et al. in the preparation of yttrium and scandium bis(*N*,*O*-bidentate salicylaldiminato) mono(alkyl) complexes which decomposed by 1,3-migration of the alkyl groups to the aldimine carbon [17]. The molecular structure of complex **3** was figured out by X-ray analysis to be seven-coordinate with a solvated THF molecule. No metal-alkyl species existed. Two ligands were bonded to the yttrium atom to form a distorted pentagonal bipyramidal geometry around the metal center (Fig. 4) with P(1), P(2), N(1), N(2) and phenoxy oxygen O(2) in equatorial positions, while the other phenoxy oxygen O(1) and the oxygen atom of THF (O(3)) axial. The bond length of N(2)–C(56) (1.321(11) Å) (Table 3) was reasonable for the normal C=N bond,

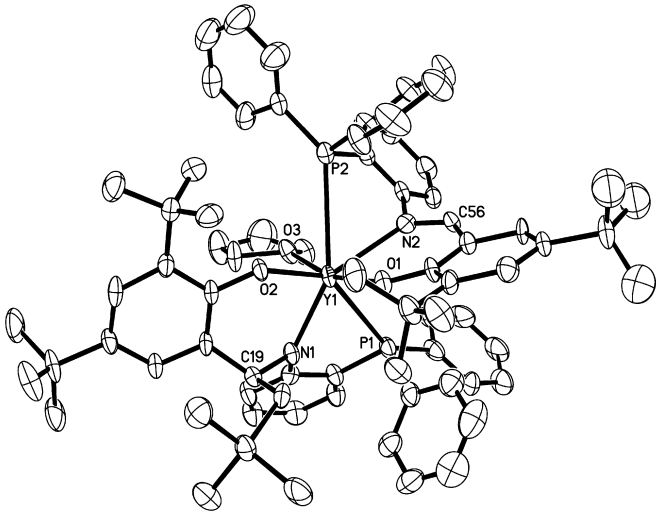

Fig. 4. X-ray structure of **3** with 35% probability of thermal ellipsoids, hydrogen atoms are omitted for clarity.

Table 3
Selected bond lengths (Å) and angles (°) for complex **3**

Y(1)–O(2)	2.130(6)	Y(1)–P(2)	3.217(3)
Y(1)–O(1)	2.162(6)	N(1)–C(18)	1.377(11)
Y(1)–N(1)	2.314(7)	N(1)–C(19)	1.468(12)
Y(1)–O(3)	2.444(7)	N(2)–C(56)	1.321(11)
Y(1)–N(2)	2.531(8)	N(2)–C(55)	1.443(11)
Y(1)–P(1)	3.040(3)		
O(2)–Y(1)–O(1)	93.9(2)	N(1)–Y(1)–P(1)	62.26(17)
O(2)–Y(1)–N(1)	81.8(2)	N(2)–Y(1)–P(1)	78.11(17)
O(1)–Y(1)–N(1)	112.3(3)	O(2)–Y(1)–P(2)	86.29(17)
O(2)–Y(1)–N(2)	138.1(2)	O(1)–Y(1)–P(2)	97.99(18)
O(1)–Y(1)–N(2)	73.5(3)	N(1)–Y(1)–P(2)	147.99(19)
N(1)–Y(1)–N(2)	140.0(2)	N(2)–Y(1)–P(2)	57.43(18)
O(2)–Y(1)–P(1)	143.50(17)	P(1)–Y(1)–P(2)	127.57(8)
O(1)–Y(1)–P(1)	94.05(17)		

meanwhile the bond length of N(1)–C(19) (1.468(12) Å) was close to the normal C–N bond (1.4904(17) Å) [13,14], indicating that C=N bond of one coordinated ligand had been reduced to a single bond via intramolecular alkylation as discussed previously for complex **2a**, while the C=N bond of another ligand retained the double bond nature. The bond distance between yttrium and the amino nitrogen $Y–N_{amino}$ (Y–N(1), 2.314(7) Å) was slightly shorter than that between yttrium and the imino nitrogen $Y–N_{imino}$ (Y–N(2), 2.531(8) Å), both fell in the range of 2.28–2.62 Å observed for Y–N bonds [18]. The six-membered ring $YO(1)N_{imino}C_3$ was planar and almost perpendicular to the six-membered ring $YO(2)N_{amino}C_3$ that was much twisted due to the flexible feature. The bond distances between the yttrium and phenoxy oxygen atoms $Y–O_{phenoxy}$ (2.130(6) Å for Y(1)–O(2) and 2.162(6) Å for Y(1)–O(1)) were much shorter than that between yttrium and the THF oxygen $Y–O_{THF}$ (Y–O(3), 2.444(7) Å). The bond angles N(2)–Y–P(2) (57.43(18)°) and N(1)–Y–P(1) (62.26(17)°) were smaller than that found in **2a** (N–Y–P, 66.54(6)°), which was contributed to the crowded environment in complex **3**.

2.1.3. Syntheses and characterization of complexes *4a* and *4b*

The β-ketoiminato ligand HL^3 with sterically bulky 2-bisphenylphosphine-phenyl group on the nitrogen was prepared, anticipated to stabilize the rare earth metal alkyl complexes and prevent the intramolecular alkyl migration and the formation of homoleptic product.

Treatment of HL^3 with 1 equiv. of $Ln(CH_2SiMe_3)_3(THF)_2$ indeed afforded mono-alkyl bis-ligand complexes $(L^3)_2Ln(CH_2SiMe_3)$ (**4a**: Ln = Y,**4b**: Ln = Lu) without alkyl migration and the formation of homoleptic counterpart (Scheme 3). X-ray diffraction analysis revealed that the complexes crystallized in the chiral triclinic space group $P\bar{1}$, and the primitive unit cell contained two independent but geometrically similar molecules. Complexes **4a** and **4b** were isostructural mono-alkyls of solvent-free stabilized by two β-ketoiminato ligands in *P*,*N*,*O*-tridentate modes. The metal centers adopted distorted pentagonal bipyramidal geometry (Figs. 5 and 6) with the enolate oxygen atoms O(1) and O(2) being axial and the N(1), N(2), P(1), P(2) and the alkyl carbon C(47) occupying the equatorial positions. The ligands coordinated to the central metal ion to form two six-membered rings $LnOC_3N$ with

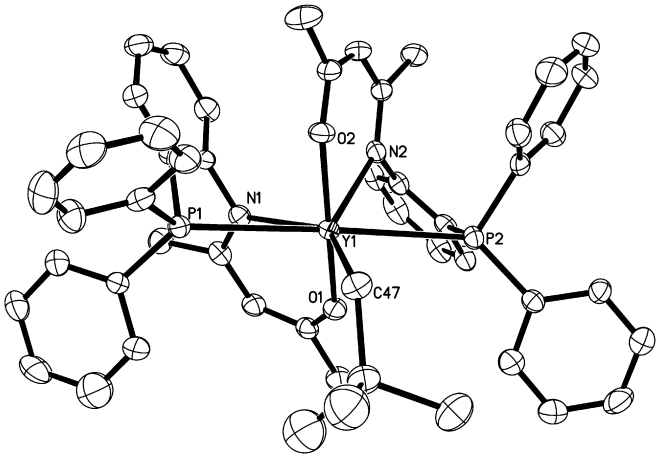

Fig. 5. X-ray structure of **4a** with 35% probability of thermal ellipsoids, hydrogen atoms are omitted for clarity.

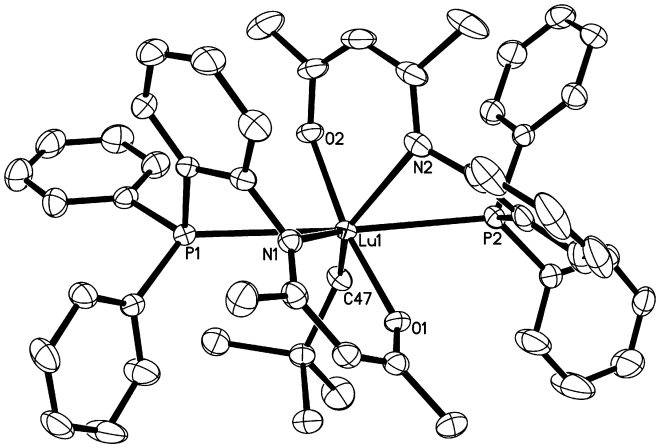

Fig. 6. X-ray structure of **4b** with 35% probability of thermal ellipsoids, hydrogen atoms are omitted for clarity.

bite angles averaging 74.53° for **4a** and 75.71° for **4b** (Table 4). The two rings arranged in *cis*-positions and both were *trans* to the metal alkyl group. The bond distances of $Ln–O_{enolate}$ (av. 2.192 Å for **4a**, and av. 2.164 Å for **4b**) were slightly longer than those of $Ln–O_{phenoxy}$ found in **2a** (2.119 Å), **2b** (2.064 Å) and **3** (av. 2.146 Å), but shorter than $Ln–O_{THF}$ (2.355–2.444 Å) in **2a**, **2b** and **3**. The Ln–N bond distances (av. 2.470(4) Å for **4a**, and av. 2.425(4) Å for

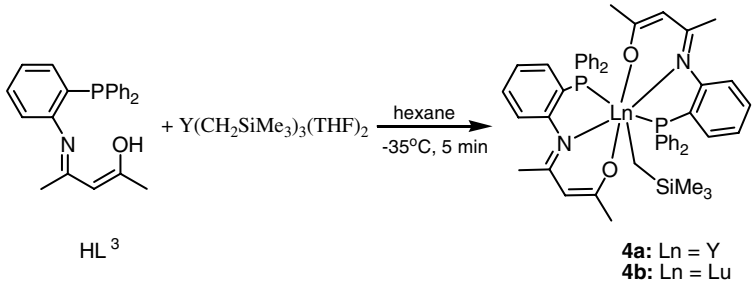

Scheme 3. Synthetic pathway for complexes **4a** and **4b**.

Table 4
Selected bond lengths (Å) and angles (°) for complexes **4a** and **4b**

	4a	4b
Ln–O(1)	2.188(3)	2.157(3)
Ln–O(2)	2.196(3)	2.170(3)
Ln–C(47)	2.427(5)	2.403(5)
Ln–N(1)	2.455(4)	2.397(4)
Ln–N(2)	2.486(4)	2.453(4)
Ln–P(2)	3.0958(13)	2.9806(12)
Ln–P(1)	3.1411(13)	3.1021(12)
O(1)–Ln–O(2)	168.29(12)	169.34(12)
O(1)–Ln–N(1)	74.64(12)	75.95(12)
O(2)–Ln–N(2)	74.42(12)	75.47(13)
N(2)–Ln–P(2)	59.48(9)	60.47(10)
N(1)–Ln–P(1)	58.93(9)	60.36(10)
P(2)–Ln–P(1)	174.35(3)	172.62(4)

4b) were slightly shorter than the corresponding Y–N_{imino} bond distance in complex **3** (2.531(8) Å) but longer than Y–N_{amino} bond distances in **2a** and **3** (av. 2.344 Å). The two phosphorus atoms located in *trans*-positions with P(1)–Ln–P(2) bond angles of 174.35(3)° for **4a** and 172.62(4)° for **4b**. The bond angles of N–Ln–P (av. 59.205° for **4a**, and av. 60.415° for **4b**) were comparable to that in complex **3** (av. 59.845°) but much smaller than the corresponding those found in **2a** (66.54°) and **2b** (69.04°).

2.1.4. Synthesis and characterization of complex 5

The above mentioned successful isolations of rare earth metal alkyl complexes supported by tridentate ligands suggested that the tetradentate bis(methoxyethylene)-amino phenol HL^4 could provide suitable electronic and steric environment to stabilize rare earth metal bis(alkyl) species.

Reaction of $Y(CH_2SiMe_3)_3(THF)_2$ with equimolar HL^4 at −35 °C for 15 min afforded a bis(alkyl) complex $(L^4)Y(CH_2SiMe_3)_2$ (**5**) as white solids in quantitative yield (Scheme 4). The ^1H NMR analysis of complex **5** displayed that the methylene protons of Y–CH_2SiMe_3 exhibited a doublet around $\delta = -0.45$ ppm, different from the singlet resonance at $\delta = -0.6$ ppm in yttrium tri(alkyl)s [19]. The isolation of single crystals from a mixture of toluene and hexane (3:1 v/v) at −35 °C allowed us figure out the molecular structure of **5** by means of X-ray analysis (Fig. 7). The complex was six-coordinate monomer without solvated THF molecule. Three carbon atoms of one *tert*-butyl group and one carbon atom of the pendent methoxy-ethylene amino fragment were disordered, and the spatial occupancy probability for each position was 50%, respectively. The two alkyl species arranged in *cis*-positions with one *endo*- and another *exo*- against the *O*,*O*,*N*,*O*-tetradentate ligand, generating a distorted tetragonal bipyramidal geometry. The phenoxy oxygen O(1), methoxy oxygen O(3), an alkyl carbon C(22) and N atoms occupied the equatorial positions, while another methoxy oxygen O(2) and another alkyl carbon C(23) atoms were axial. The bond angle formed by yttrium ion and pendent methoxy oxygen atoms O(2)–Y–O(3) was 76.96(7)°, whereas O(11)–Co–O(15) was 121.31(4)° for a cobalt complex supported by analogous phenolate ligand [20]. The distances between yttrium atom and the pendent methoxy oxygen atoms Y–$O_{methoxy}$ (Y–O(2), 2.513(2) Å; Y–O(3), 2.4149(19) Å) were comparable to those of Y–O_{THF} and Y–O_{ether} in a range of 2.45–2.50 Å [21,22], but longer than the distance between yttrium atom and the phenoxy oxygen atom Y–$O_{phenoxy}$ (Y–O(1), 2.1179(19) Å) (Table 5), indicating the similar bond strength of Y–$O_{methoxy}$ and Y–O_{THF}. The bond length of Y–N (2.507(3) Å) was comparable to those found in complexes **2a**, **2b**, **3** and **4a**, **4b** (2.374–2.486 Å). The bond angles $O_{methoxy}$–Y–N averaging 67.945° were also close to the corresponding those found in a yttrium dialkyl complex $[(CH_3OCH_2CH_2)_2NCH_2\text{-}3,5\text{-}(CMe_3)_2\text{-}2\text{-}C_6H_2O]Y(CH_2\text{-}SiMe_2Ph)_2$ (65.89(4)–69.30(4)°) [23]. The bond angle $O_{phenoxy}$–Y–N (78.21(8)°) was comparable to the corresponding data in a phenoxytriamine yttrium complex

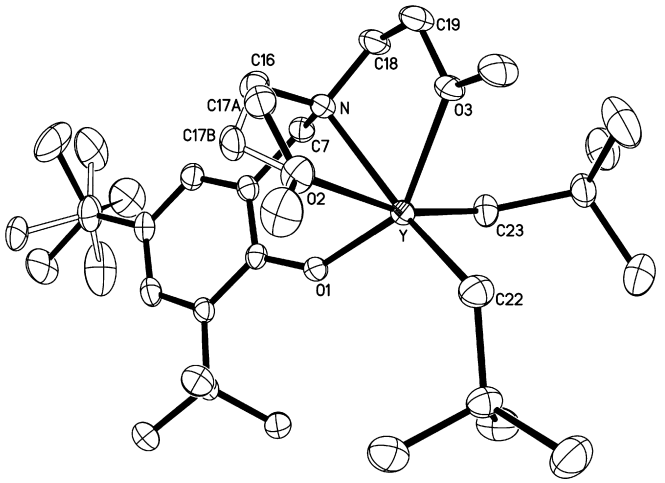

Fig. 7. X-ray structure of **5** with 35% probability of thermal ellipsoids, hydrogen atoms are omitted for clarity.

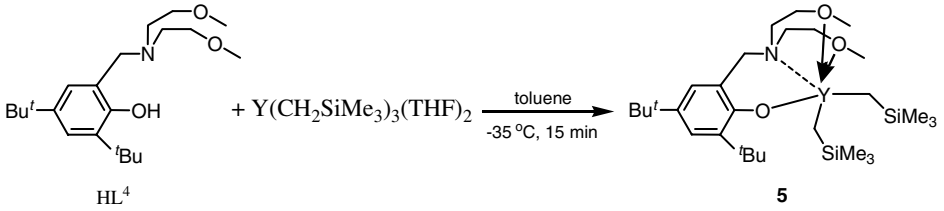

HL^4 **5**

Scheme 4. Synthetic pathway for complex **5**.

Table 5
Selected bond lengths (Å) and angles (°) for complex **5**

Y–C(22)	2.425(4)	Y–O(1)	2.1179(19)
Y–C(23)	2.421(3)	Y–O(2)	2.513(2)
Y–N	2.507(3)	Y–O(3)	2.4149(19)
O(1)–Y–C(23)	97.29(9)	O(1)–Y–O(3)	146.26(7)
O(3)–Y–C(23)	92.91(9)	O(1)–Y–O(2)	84.78(8)
O(1)–Y–C(22)	115.39(10)	O(3)–Y–O(2)	76.96(7)
O(3)–Y–C(22)	93.58(10)	C(23)–Y–O(2)	163.44(10)
C(23)–Y–C(22)	101.93(12)	C(22)–Y–O(2)	91.87(11)
O(1)–Y–N	78.21(8)	O(2)–Y–N	67.25(8)
O(3)–Y–N	68.64(8)	O(2)–C(17A)–C(16)	112.5(5)
C(23)–Y–N	96.99(10)	O(2)–C(17B)–C(16)	113.1(7)
C(22)–Y–N	154.70(10)		

(O(1)–Y–N(1), 76.2(2)°) [10], but smaller than those found in complexes **2a** (85.69(8)°) and **2b** (88.15(16)°). The bond lengths and angle formed by alkyl species with metal ion, Y–C (av. 2.423 Å) and C–Y–C (101.93(12)°) were within the reasonable ranges found in other bis(alkyl) complexes bearing heteroatom-containing ligands [24].

2.2. Ring-opening polymerization of L-lactide

Rare earth metal complexes **2a**, **2b**, **4a**, **4b** and **5** were active initiators for the ring-opening polymerization (ROP) of L-lactide (L-LA) under mild conditions. The catalytic activity was dependent on the molecular structures of the complexes and the polymerization conditions. The representative polymerization data were summarized in Tables 6–8. When mono(alkyl) complexes **2a**,**b** and **5** being initiators, complete conversions of the monomer into polylactide (PLA) were achieved within 2 h at 20 °C, whereas only 1 h was needed when complexes **4a** and **4b** being initiators at the same conditions. This might be attributed to the coordination of two THF molecules in complexes **2a**,**b**. The less reactive characteristic of complex **5** might be due to the coordination of methoxy moieties which played similar roles as those of THF moieties in complexes **2a**,**b**.

At various monomer-to-initiator ratios ranging from 100 to 1000, polymerization of L-LA initiated by complexes **2a** and **5** proceeded smoothly at 20 °C. The molecular weight of the resulting PLA increased with the ratio while the molecular weight distribution kept no change obviously, indicating that the reaction was controllable. When the ratio was raised over 500, the polymerization was sluggish because of the lower concentration of the initiator, and complete conversion could not be reached even for long reaction time. Generally, the molecular weight of the resultant PLA was lower than the theoretic value. In the case of bis(alkyl) complex **5** being the initiator, molecular weight of PLA was halved compared with those when using mono(alkyl) complexes as initiators, suggesting that both metal alkyl species participated in the initiation, namely, double-sites, leading to the relatively broader molecular weight distribution (Table 7).

Table 6
Polymerization of L-lactide with various rare earth meta alkyl complexes[a]

Entry	Catalyst	t (h)	$M_n \times (10^{-4})$[b]	M_w/M_n
1	**2a**	2	2.00	1.46
2	**2b**	2	2.12	1.47
3	**4a**	1	1.97	1.45
4	**4b**	1	2.05	1.48
5	**5**	2	1.59	1.65

[a] Solvent: THF, 20 °C, [L-LA]: 1.0 mol/L, [LA]/[Ln] = 300.
[b] Measurement by GPC calibrated with polystyrene standard and corrected using a factor of 0.58.

Table 7
Polymerization of L-lactide at different monomer-to-initiator ratios[a]

Entry	Catalyst	[LA] /[Y]	Conversion (%)[b]	M_n (10^{-4})[c]	M_w/M_n[c]
1	**2a**	100	99.6	1.00	1.43
2	**2a**	200	97.8	1.56	1.46
3	**2a**	300	98.6	2.00	1.46
4	**2a**	500	97.1	5.37	1.39
5	**2a**	700	95.5	7.44	1.45
6	**2a**	1000	90.2	12.9	1.26
7	**5**	300	98	1.59	1.65
8	**5**	500	96	2.4	1.64
9	**5**	700	95	3.63	1.58
10	**5**	1000	88	6.0	1.59

[a] Solvent THF, [L-LA] = 1.0 mol/L, 20 °C, 2 h.
[b] Weight of polymer obtained/weight of monomer used.
[c] Measurement by GPC calibrated with standard polystyrene samples, and corrected using a factor 0.58.

Table 8
Influence of the reaction medium on the polymerization of L-lactide[a]

Entry	Solvent	[L-LA]/[Y]	t (h)	Conversion (%)[b]	M_n (10^{-4})[c]	M_w/M_n[c]
1	THF	300	2	98	1.59	1.65
2	CH_2Cl_2	300	5	31	n.d.	n.d.
3	Toluene	300	2	82	1.21	1.42

[a] Complex **5**, [L-LA]: 1.0 mol/L, 20 °C.
[b] Weight of polymer obtained/weight of monomer used.
[c] Measurement by GPC calibrated with standard polystyrene samples, and corrected using a factor 0.58.

Reaction medium played important role in the polymerization. THF was the most optimum solvent (Table 8). In contrast, when the polymerization was performed in CH_2Cl_2, the conversion was only 31% for long time (5 h). This could be imputed to the coordination of CH_2Cl_2 which changed the steric environment and the Lewis acidity of the central metal [25], consistent with the previously reported bis(phenolate)yttrium system [26]. When using toluene as medium, the conversion was relatively higher than in CH_2Cl_2 but still lower than in THF due to the poor solubility of L-LA in toluene.

The ^{1}H NMR spectrum of PLA displayed a symmetric quartet resonance at $\delta = 5.15$ ppm assigned to the methine proton, indicating the isotactic microstructure of PLA. No racemization was detectable.

The ^{1}H NMR spectrum of PLA oligomer (complex **2a**, $[LA]_0/[Y]_0 = 20$) displayed signals at $\delta = 4.35$, 2.66,

1.48 ppm assigned to the end group $HOCH(CH_3)CO$– [26b,27]. The resonances for the other end group –$COCH_2SiMe_3$ derived from the coordination-insertion of LA into metal alkyl species Ln–CH_2SiMe_3, was weak, whereas, the end group –$COOCH_3$ gave strong resonance around $\delta = 3.74$ ppm. This might be imputed to the unstable nature of –$COCH_2SiMe_3$ that swiftly transferred into –$COOCH_3$ due to the exchange reaction with terminator CH_3OH, in agreement with the previously reported result [28].

3. Conclusion

We have demonstrated the syntheses and structures of several lanthanide mono- or bis-alkyl complexes stabilized by multidentate phenoxide ligands. The protonolysis reaction along with intramolecular alkylation of the C=N bond of the ligand were observed in some cases. Both the molecular structure and the catalytic performance are strongly dependent on the ligand framework. The di-ligand chelated momo(alkyl) complexes were more active toward the ROP of L-LA than the mono-ligand chelated momo(alkyl) complexes of two THF solvate and the bis(alkyl) complex coordinated by two methoxy moieties, indicating that the electron-negative metal center decreased the catalytic activities of the corresponding complexes.

4. Experimental

4.1. General methods

All the syntheses and manipulations of air- and moisture-sensitive materials were carried out under a dry and oxygen-free argon atmosphere by using Schlenk techniques or under a nitrogen atmosphere in an MBRAUN glovebox. All solvents were purified from MBRAUN SPS system. Organometallic samples for NMR spectroscopic measurements were prepared in a glovebox by using NMR tubes sealed with paraffin film. ^1H, ^{13}C NMR spectra were recorded on a Bruker AV400 (400 MHz for ^1H, 100 MHz for ^{13}C) spectrometer. NMR assignments were confirmed by the ^1H–^1H (COSY) and ^1H–^{13}C (HMQC) experiments when necessary. IR spectra were recorded on a VERTEX 70 FT-IR spectrometer. Gel permeation chromatography (GPC) analyses of polymer samples were carried at 30 °C using THF as an eluent on a Waters-410 instrument and calibrated using polystyrene standards. Elemental analyses were performed at National Analytical Research Centre of Changchun Institute of Applied Chemistry (CIAC). L-LA (Aldrich) was recrystallized from $CH_3COOCH_2CH_3$ was dried over CaH_2, distilled before use. (2-Diphenylphosphino) aniline was prepared according to the literature [29].

4.2. Syntheses of complexes

4.2.1. Syntheses of ligands

Tridentate ligands 3,5-^{t}Bu$_2$-$(OH)C_6H_2CH$=N-$CH_2CH_2NMe_2$ (HL^1) and 3,5-^{t}Bu$_2$-$(OH)C_6H_2CH$=N-2-$PPh_2C_6H_4$(HL^2) were synthesized according to the literatures [13,30] by Schiff-base condensation from 3,5-^{t}Bu$_2$-$(OH)C_6H_2CHO$ and the corresponding amino derivatives. Phosphino β-ketoimine, 2-$PPh_2C_6H_4N$=$C(Me)CH_2C(O)CH_3$ (HL^3) was prepared in good yields by condensation of the corresponding β-diketone with (2-diphenylphosphine)aniline in methanol [13,30]. The tetradentate ligand HL^4 was prepared from 2,4-^{t}Bu$_2$-C_6H_2OH, paraformaldehyde and $(MeOCH_2CH_2)_2NH$ in refluxing methanol via Mannich condensation [10].

4.2.2. Synthesis of complex *1*

A solution of HL^1 (0.123 g, 0.04 mmol) in hexane (6 mL) was added dropwise to a hexane solution of $Y(CH_2SiMe_3)_3(THF)_2$ (0.20 g, 0.40 mmol) at −35 °C. The resulting orange mixture was stirred overnight at room temperature, and then the volatile was removed in vacuum. The residue was washed with hexane to afford orange-yellow solids of complex **1** (0.20 g, 51%). Single crystals suitable for X-ray analysis grew from a hexane solution of **1** cooled to −35 °C for several days. ^1H NMR (400 MHz, C_6D_6, 25 °C): δ 1.47 (s, 27H, ^{t}Bu), 1.73 (s, 27H, ^{t}Bu), 2.15 (br, 18H, NMe_2), 2.53 (br, 6H, CH_2NMe_2), 3.60 (br, 6H, $CH_2CH_2NMe_2$), 7.25 (s, 3H, Ar*H*), 7.73 (s, 3H, Ar*H*), 8.29 (br, 3H, C*H*=N). ^{13}C NMR (100 MHz, C_6D_6, 25 °C): δ 30.60 (s, 9C, ^{t}*Bu*), 32.31 (s, 9C, ^{t}*Bu*), 34.50 (s, 3C, *C*Me_3), 35.99 (s, 3C, *C*Me_3), 46.29 (br, 6C, NMe_2), 47.37 (s, 3C, *C*H_2NMe_2), 60.79 (s, 3C, *C*$H_2CH_2NMe_2$), 123.05 (s, 3C, *p*-OC_6H_2), 130.04 (t, 3C, *o*-N=CC_6H_2), 130.73 (s, 3C, *p*-N=CC_6H_2), 136.48 (s, 3C, *o*-OC_6H_2), 139.68 (s, 3C, *ipso*-N=CC_6H_2), 165.18 (s, 3C, *ipso*-OC_6H_2), 171.72 (s, 3C, *C*H=N); IR (KBr pellets): 638, 703, 745, 788, 814, 838, 876, 900, 929, 978, 1025, 1079, 1164, 1201, 1236, 1257, 1274, 1325, 1359, 1415, 1439, 1462, 1535, 1615, 2767, 2867, 2955 cm^{-1}. Anal. Calc. for $C_{58.50}H_{96.50}N_6O_3Y$: C, 67.76; H, 9.16; N, 8.78. Found: C, 67.58; H, 9.03; N, 8.47%.

4.2.3. Synthesis of complex *2a*

A solution of HL^2 (0.20 g, 0.40 mmol) in hexane (5 mL) was added dropwise to a hexane solution of $Y(CH_2SiMe_3)_3(THF)_2$ (0.20 g, 0.400 mmol) at −35 °C. The yellow reaction mixture was stirred for 30 min and then concentrated under reduced pressure to afford yellow solids which were washed with cold hexane (2 mL × 3) to give **2a** (0.28 g, 78%). Single crystals suitable for X-ray analysis grew from a cold hexane solution of **2a** at −35 °C within several days. ^1H NMR (400 MHz, C_6D_6, 25 °C): δ −0.39 (AB, 2H, $^2J_{H-H} = 11.2$ Hz, $J_{H-Y} = 2$ Hz , YCH_2SiMe_3), 0.06 (s, 9H, CH_2SiMe_3), 0.55 (s, 9H, $CHCH_2SiMe_3$), 1.14 (s, 8H, THF), 1.21 (d, 1H, $^2J_{H-H} = 12$ Hz, $^3J_{H-H} = 4$ Hz, $CHCH_2SiMe_3$), 1.53 (s, 9H, ^{t}*Bu*), 1.88 (s, 9H, ^{t}*Bu*), 2.08 (t, 1H, $^3J_{H-H} = 13.6$ Hz, $^3J_{H-H} = 12.8$ Hz, $CHCH_2SiMe_3$), 3.75 (s, 8H, THF), 4.82 (d, 1H, $^3J_{H-H} = 10.8$ Hz, C*H*CH_2SiMe_3), 6.50 (t, 1H, $^3J_{H-H} = 7.2$ Hz, *m*-PC_6H_4N), 7.07–7.16 (m, 8H, *m*,*p*-PC_6H_5, *m*-NC_6H_4P,C_6H_2), 7.47–7.50 (m, 3H,

o-PC_6H_4N, *o*-NC_6H_4P and C_6H_2), 7.72–7.67 (m, 4H, *o*-PC_6H_5). ^{13}C NMR (100 MHz, C_6D_6, 25 °C): δ −0.60 (s, 3C, CHSi*Me*$_3$), 5.57 (s, 3C, CH_2Si*Me*$_3$), 25.37 (s, 8C, THF), 26.09 (s, 2C, Y*C*H_2), 31.11 (s, 3C, ^{t}*Bu*), 32.71 (s, 3C, ^{t}*Bu*), 34.71 (s, 1C, *C*Me$_3$), 36.28 (s, 1C, *C*Me$_3$), 64.08 (s, 1C, *C*HCH_2SiMe_3), 71.38 (s, 8C, THF), 111.84 (s, 1C, *p*-PC_6H_4N), 112.97 (s, 1C, *p*-NC_6H_4P), 115.18 (d, 1C, *ipso*-PC_6H_4), 122.36 (s, 1C, *o*-NC_6H_4P), 125.80 (s, 1C, *o*-PC_6H_4N), 128.95, 129.24 (d, 4C, *m*-PC_6H_5), 129.91 (d, 2C, *ipso*-PC_6H_5), 134.18 (s, 1C, *m*-OC_6H_2), 134.40 (d, 2C, *p*-PC_6H_5), 134.99 (2C, *o*,*m*-OC_6H_2), 135.37 (d, 4C, *o*-C_6H_5), 136.97 (s, 1C, *p*-OC_6H_2), 137.85 (s, 1C, *o*-OC_6H_2-^{t}Bu), 159.98 (s, 1C, *ipso*-NC_6H_4), 164.66 (d, 1C, *ipso*-OC_6H_2); IR (KBr pellets): 696, 730, 745, 791, 841, 918, 998, 1028, 1069, 1097, 1136, 1163, 1193, 1250, 1330, 1361, 1386, 1436, 1461, 1533, 1596, 1612, 2869, 2904, 2955, 3056 cm^{-1}. Anal. Calc. for $C_{49}H_{73}NO_3PSi_2Y$: C, 65.38; H, 8.17; N, 1.56. Found: C, 65.41; H, 8.19; N, 1.54%.

4.2.4. Synthesis of complex *2b*

Following the same procedure described for the synthesis of **2a**, treatment of HL^2 (0.20 g, 0.40 mmol in 5 mL hexane) with $Lu(CH_2SiMe_3)_3(THF)_2$ (0.23 g, 0.40 mmol) afforded yellow solids of **2b** (0.32 g, 80%). Single crystals suitable for X-ray analysis grew from a cold solution of complex **2b** in hexane/toluene (1:3 v/v) at −35 °C within several days.^1H NMR (400 MHz, C_6D_6, 25 °C): δ −0.47 (d, 1H, LuC*H*$_2$SiMe$_3$), 0.06 (s, 9H, LuCH$_2$Si*Me*$_3$), 0.56 (s, 9H, CHCH$_2$Si*Me*$_3$), 1.11 (br, 8H, THF), 1.54 (s, 9H, ^{t}*Bu*), 1.86 (s, 9H, ^{t}*Bu*), 2.35 (t, 1H, LuC*H*$_2$SiMe$_3$), 3.70 (br, 8H, THF), 4.98 (d, 1 H, $^3J_{H-H} = 14$ Hz, C*H*CH$_2$-SiMe$_3$), 6.55 (t, 1H, *m*-PC_6H_4N), 7.04–7.11 (m, 2H, *o*-NC_6H_4P,C_6H_2), 7.15–7.23 (m, 5H, *m*-PC_6H_5, *o*-PC_6H_4N), 7.49–7.56 (m, 4H, *p*-P-C_6H_5, *m*-NC_6H_4P and C_6H_2), 7.81–7.85 (m, 4H, *o*-PC_6H_5). ^{13}C NMR (100 MHz, C_6D_6, 25 °C): δ −0.68 (s, 3C, CHSi*Me*$_3$), 5.35 (s, 3C, CH_2Si*Me*$_3$), 25.37 (s, 8C, THF), 25.78 (s, 2C, Y*C*H_2), 31.18 (s, 3C, ^{t}*Bu*), 32.71 (s, 3C, ^{t}*Bu*), 34.71 (s, 1C, *C*Me$_3$), 36.22 (s, 1C, *C*Me$_3$), 63.16 (s, 1C, *C*HCH_2SiMe_3), 71.56 (s, 8C, THF), 112.25 (s, 1C, *m*-NC_6H_4P), 113.36 (s, 1C, *p*-NC_6H_4P), 114.19 (d, 1C, *ipso*-PC_6H_4), 122.46 (s, 1C, *ipso*-NC_6H_4), 125.69 (s, 1C, *o*-PC_6H_4N), 129.23, 129.31 (d, 4C, *m*-PC_6H_5), 129.73,130.38 (s, 2C, *ipso*-PC_6H_5), 134.18 (s, 1C, C_6H_2), 134.40 (d, 2C, *p*-PC_6H_5), 134.99 (2C, *o*,*m*-NC_6H_2), 135.37 (d, 4C, *o*-C_6H_5), 137.18 (s, 1C, *p*-OC_6H_2), 138.09 (s, 1C, *o*-OC_6H_2-^{t}Bu), 160.47 (s, 1C, *ipso*-NC_6H_4), 165.08 (d, 1C, *ipso*-OC_6H_2); IR (KBr pellets): 696, 744, 791, 841, 918, 999, 1027, 1066, 1094, 1137, 1163, 1191, 1256, 1331, 1360, 1385, 1435, 1460, 1533, 1595, 1612, 2868, 2956, 3054 cm^{-1}. Anal. Calc. for $C_{49}H_{73}NO_3PSi_2Lu$: C, 59.62; H, 7.45; N, 1.42. Found: C, 59.71; H, 7.69; N, 1.54%.

4.2.5. Synthesis of complex *3*

A solution of HL^2 (0.40 g, 0.8 mmol) in hexane (5 mL) was added dropwise to 0.5 equiv. of $Y(CH_2SiMe_3)_3(THF)_2$ (0.20 g, 0.4 mmol) in hexane at −35 °C. The red solution was stirred for 12 h at room temperature. Removal of volatiles afforded red solids which were recrystallized from hexane to produce complex **3** (0.37 g, 75%). Orange crystals suitable for X-ray analysis grew by cooling a hexane solution of complex **3** to −35 °C for several days. ^1H NMR (400 MHz, C_6D_6, 25 °C): δ −0.33 (s, 2H, C*H*$_2$SiMe$_3$), −0.03 (s, 9H, YCH$_2$Si*Me*$_3$), 0.08 (s, 9H, CHCH$_2$Si*Me*$_3$), 1.29 (s, 4H, THF), 1.14 (d, 1H, $J = 12$ Hz, CHC*H*$_2$SiMe$_3$), 1.36 (s, 18H, ^{t}*Bu*), 1.56 (s, 18H, ^{t}*Bu*), 2.01 (t, 1H , $J = 12$ Hz, CHC*H*$_2$SiMe$_3$), 3.60 (s, 4H, THF), 4.94 (d, 1H, $J = 11.6$ Hz, C*H*CH$_2$SiMe$_3$), 6.88–7.00 (m, 2H, *m*-PC_6H_4N), 7.14–7.22 (m, 16H, *m*,*p*-PC_6H_5,*m*-NC_6H_4P,C_6H_2), 7.33–7.45 (m, 6H, *o*-PC_6H_4N, *o*-NC_6H_4P and C_6H_2), 7.60–7.74 (m, 8H, *o*-PC_6H_5), 7.90 (s, 1H, C*H*=N). ^{13}C NMR (100 MHz, C_6D_6, 25 °C): δ −0.52 (s, 3C, CHCH$_2$Si*Me*$_3$), 14.77 (s, 1C, CH*C*H$_2$Si*Me*$_3$), 25.89 (s, 4C, THF), 23.47 (s, 1C, Y*C*H_2), 31.26 (s, 1C, Y*C*H$_2$SiMe$_3$), 32.15 (s, 4C, ^{t}*Bu*), 32.80 (s, 4C, ^{t}*Bu*), 34.70 (d, 2C, $J = 23.3$ Hz, *C*Me$_3$), 36.14 (d, 2C, $J = 17.5$ Hz *C*Me$_3$), 64.32 (s, 1C, *C*HCH$_2$SiMe$_3$), 69.47 (s, 8C, THF), 122.07 (s, 2C, *p*-PC_6H_4N), 122.56 (s, 2C, *p*-NC_6H_4P), 122.88 (d, 2C, *ipso*-PC_6H_4), 123.64 (s, 2C, *o*-NC_6H_4P), 124.86 (s, 2C, *o*-PC_6H_4N), 127.07, 129.19 (d, 8C, *m*-PC_6H_5), 129.75 (d, 4C, *ipso*-PC_6H_5), 132.33 (s, 1C, *C*H=N), 132.33 (s, 2C, *m*-OC_6H_2), 133.32 (d, 4C, *p*-PC_6H_5), 133.92 (m, 4C, *o*,*m*-OC_6H_2), 135.42 (m, 8C, *o*-C_6H_5), 136.68 (s, 2C, *p*-OC_6H_2), 137.69 (s, 2C, *o*-OC_6H_2-^{t}Bu), 157.29 (s, 2C, *ipso*-NC_6H_4), 165.11 (d, 2C, *ipso*-OC_6H_2); IR (KBr pellets): 696, 743, 766, 790, 841, 918, 999, 1027, 1068, 1094, 1163, 1193, 1249, 1275, 1329, 1360, 1388, 1435, 1461, 1479, 1532, 1591, 1609, 2867, 2905, 2955, 3054, 3211, 3668 cm^{-1}. Anal. Calc. for $C_{74}H_{89}N_2O_3P_2SiY$: C, 72.06; H, 7.27; N, 2.27. Found: C, 72.29; H, 7.35; N 2.31%.

4.2.6. Synthesis of complex *4a*

To a hexane solution (5.0 mL) of $Y(CH_2SiMe_3)_3(THF)_2$ (0.15 g, 0.30 mmol), 1 equiv. of HL^3 (0.13 g, 0.30 mmol in 4 mL toluene) was dropwise added at −35 °C under stirring, and the reaction was kept at −35 °C for 5–10 min. Removal of the volatiles gave deep red solids, which were dissolved in 1 mL toluene, and cooled to −35 °C for 2 days to give colorless crystalline solids. Washed with hexane carefully and dried *in vacuum* afforded complex **4a** (0.10 g, 35%). Single crystals suitable for X-ray analysis grew from a toluene solution of **4a** at −35 °C for several days. ^1H NMR (400 MHz, C_6D_6, 25 °C): δ −0.33 (s, 2H, C*H*$_2$SiMe$_3$), 0.51 (s, 9H, Si*Me*$_3$), 1.25 (s, 3H, C*H*$_3$C=N), 1.71(s, 3H, C*H*$_3$CO), 4.53 (s, 2H, COC*H*C=N), 6.64 (br, 2H, *o*-PC_6H_4N), 6.91 (br, 2H, *o*-NC_6H_4P), 7.10–7.17 (m, 10H, *m*,*p*-PC_6H_5, *m*,*p*-NC_6H_4P), 7.34 (br, 6H, *m*,*p*-PC_6H_5), 7.70 (br, 4H, *o*-PC_6H_5), 8.15 (br, 4H, *o*-PC_6H_5). ^{13}C NMR (100 MHz, C_6D_6, 25 °C): δ 5.81 (3C, Si*Me*$_3$), 22.96 (2C, *C*H$_3$C=N), 26.3 (s, 2C, C*H*$_3$C-O), 101.41 (s, 2C, *C*H), 124.43 (2C, *o*-PC_6H_4N), 124.64 (2C, *o*-NC_6H_4P), 129.14 (6C, *m*,*p*-PC_6H_5), 130.22 (10C, *m*,*p*-PC_6H_5, *m*,*p*-NC_6H_4P), 131.73 (s, 2C, *ipso*-PC_6H_4), 135.49 (2C,

o-PC_6H_5), 135.74 (t, 2C, *o*-PC_6H_5), 153.37 (s, 2C, *ipso*-NC_6H_4), 169.14 (s, 2C, *C*=N), 179.58 (s, 2C, *C*-O); IR (KBr pellets): 696, 743, 819, 862, 930, 1013, 1068, 1094, 1123, 1157, 1188, 1235, 1262, 1404, 1434, 1457, 1511, 1576, 2954, 3052 cm^{-1}. Anal. Calc. for $C_{57}H_{61}N_2O_2P_2SiY$: C, 69.50; H, 6.24; N, 2.84. Found: C, 69.52; H, 6.25; N, 2.80%.

4.2.7. Synthesis of complex **4b**

To a hexane solution (5.0 mL) of $Lu(CH_2SiMe_3)_3(THF)_2$ (0.18 g, 0.30 mmol), 1 equiv. of HL^3 (0.13 g, 0.31 mmol in 4 mL toluene) was dropwise added at −35 °C, and the reaction was kept at −35 °C for 5–10 min. Removal of the volatiles gave deep red solids, which was dissolved in 3 mL toluene and concentrated to 1 mL, then cooled to −35 °C for 2 days to give colorless crystals of complex **4b** (0.11g, 33%). Single crystals suitable for X-ray analysis grew from a toluene solution of **4b** at −35 °C for several days. ^{1}H NMR (400 MHz, C_6D_6, 25 °C): δ −0.45 (br, 2H, CH_2SiMe$_3$), 0.49 (s, 9H, SiMe_3), 1.24 (s, 3H, CH_3C=N), 1.72 (s, 3H, CH_3C–O), 4.51 (s, 2H, CH), 6.64 (br, 2H, *o*-PC_6H_4N), 6.97 (br, 2H, *o*-NC_6H_4P), 7.11–7.17 (m, 10H, *m*,*p*-PC_6H_5, *m*,*p*-NC_6H_4P), 7.33 (br, 6H, *m*,*p*-PC_6H_5), 7.71 (br, 4H, *o*-PC_6H_5), 8.15 (br, 4H, *o*-PC_6H_5). ^{13}C NMR (100 MHz, C_6D_6, 25 °C): δ 5.95 (3C, SiMe_3), 23.09 (2C, *C*H$_3$C=N), 26.33 (s, 2C, CH$_3$*C*–O), 101.75 (s, 2C, CO*C*HCN), 124.45 (2C, *o*-PC_6H_4N), 124.72 (2C, *o*-NC_6H_4P), 129.07 (6C, *m*,*p*-PC_6H_5), 130.15 (10C, *m*,*p*-PC_6H_5, *m*,*p*-NC_6H_4P), 131.64 (s, 2C, P–C_6H_4), 135.45 (2C, *o*-PC_6H_5), 135.88 (t, 2C, $J_{P-C} = 12$ Hz, *o*-PC_6H_5), 153.41 (s, 2C, N–C_6H_4), 169.12 (s, 2C, *C*=N), 179.96 (s, 2C, *C*–O); IR (KBr pellets): 696, 743, 821, 861, 932, 1015, 1086, 1097, 1124, 1157, 1189, 1235, 1264, 1400, 1435, 1457, 1512, 1578, 2953, 3053 cm^{-1}. Anal. Calc. for $C_{57}H_{61}N_2O_2P_2SiLu$: C, 63.92; H, 5.74; N, 2.62. Found: C, 63.95; H, 5.75; N, 2.60%.

4.2.8. Synthesis of complex **5**

A toluene (2 mL) solution of HL^4 (0.18 g, 0.52 mmol) was added dropwise to 1 equiv. of $Y(CH_2SiMe_3)_3(THF)_2$ (0.26 g, 0.52 mmol) in toluene (2 mL) at −35 °C. The reaction mixture was stirred for 15 min and then concentrated in vacuo to 1 mL. Crude product was precipitated as white solids, which was washed with hexane carefully and dried in vacuum to afford complex **5** (0.28 g, 78%). Colorless single crystals for X-ray analysis grew from a mixture of toluene and hexane (3:1 v/v) at −35 °C within 4 days. ^{1}H NMR (400 MHz, C_6D_6, 25 °C): δ −0.45 (d, 4H, $J = 2.8$ Hz, YCH_2SiMe$_3$), 0.58 (s, 18H, YCH$_2$SiMe_3), 1.53 (s, 9H, CMe_3), 1.64 (t, 2H, $J = 12$ Hz, NCH_2CH$_2$OMe), 1.92 (s, 9H, CMe_3), 2.56 (m, 2H, NCH$_2$*C*H$_2$OMe), 2.56 (m, 2H, N*C*H$_2$CH$_2$OMe), 2.87(t, 2H, $J = 16$ Hz, NCH$_2$CH_2OMe), 3.18 (s, 6H, OMe), 3.56 (s, 2H, CH_2N), 7.02 (d, 1H, $J = 4$ Hz, ArH), 7.69 (d, 1H, $J = 4$ Hz, ArH); ^{13}C NMR (100 MHz, C_6D_6, 25 °C): δ 5.23 (s, 6C, CH$_2$SiMe_3), 30.77 (s, 3C, CMe_3), 31.11 (s, 2C, *C*H$_2$SiMe$_3$), 32.68 (s, 3C, CMe_3), 34.70 (s, 1C, *C*Me$_3$), 36.15 (s, 1C, *C*Me$_3$), 52.86 (s, 2C, N*C*H$_2$CH$_2$), 61.49 (s, 2C, OMe), 63.90 (s, 1C, *C*H$_2$N), 72.10 (s, 2C, CH$_2$*C*H$_2$OMe), 123.61, 125.26, 126.01, 137.07, 137.47, 162.53 (s, 6C, *aryls*); IR (KBr pellets): 616, 644, 669, 694, 744, 840, 861, 877, 1028, 1091, 1114, 1166, 1202, 1248, 1309, 1321, 1361, 1383, 1416, 1442, 1478, 1545, 1604, 2900, 2953, 3418, 3676 cm^{-1}. Anal. Calc. For $C_{29}H_{58}NO_3Si_2Y$: C, 56.74; H, 9.52; N, 2.28. Found: C, 56.71; H, 9.56; N, 2.29%.

4.3. Polymerization of L-lactide

4.3.1. Typical procedure for polymerization of L-lactide

A typical procedure for polymerization of lactide was performed in a 25 mL round-bottom flask in a glove-box. To a stirred THF solution (3.0 mL) of L-lactide (0.50 g, 3.47 mmol) was added a THF solution (1.0 mL) of complex **5** (4.58 mg, 6.94 μmol, $[LA]_0/[Cat]_0 = 500$) (Table 7, entry 8). The polymerization was proceeded for 2 h at room temperature (20 °C) and then terminated by 1.0 mL of a mixture of $HCl/CH_3OH/CHCl_3$ (1:100:600 v:v) to give white solids, which were filtered, washed with ethanol, and then dried at 40 °C for 24 h in vacuo to give PLA (0.48 g, 96%). The molecular weight and the molecular weight distribution of the resulting polymer were determined by GPC. The microstructure was characterized by ^{1}H NMR spectrum.

4.3.2. Oligomer for NMR measurement

To the stirred solution of L-lactide (0.125 g, 0.87 mmol) in THF (1.5 mL), the solution of complex **2a** (41 mg, 0.046 mmol) in THF (0.5 mL) was injected at 20 °C ($[LA]_0/[Y]_0 = 20$). The polymerization mixture was stirred for 2 h and then quenched with hexane/methanol (1:1 v:v). The precipitated oligomer was collected and dried and used for ^{1}H NMR.

4.4. X-ray crystallographic studies

Crystals for X-ray analysis were obtained as described in the preparations. The crystals were manipulated in the glovebox. Data collections were performed at −86.5 °C on a Bruker SMART APEX diffractometer with a CCD area detector, using graphite-monochromated Mo Kα radiation ($\lambda = 0.71073$ Å). The determination of crystal class and unit cell parameters was carried out by the SMART program package. The raw frame data were processed using SAINT and SADABS to yield the reflection data file. The structures were solved by using the SHELXTL program. Refinement was performed on F^2 anisotropically for all non-hydrogen atoms by the full-matrix least-squares method. The hydrogen atoms were placed at the calculated positions and were included in the structure calculation without further refinement of the parameters. The crystallographic data and the refinement of complexes **1**, **2a**, **2b**, **3**, **4a**, **4b**, **5** are summarized in Tables 9 and 10, respectively.

Table 9
Summary of crystallographic data for **1**, **2a**, **2b**, and **3**

	1	**2a**	**2b**	**3**
Formula	$C_{58.50}H_{96.50}N_6O_3Y$	$C_{49}H_{73}NO_3PSi_2Y$	$C_{49}H_{74}NO_3Si_2PLu$	$C_{74}H_{89}N_2O_3P_2SiY$
Molecular weight	1020.83	900.14	987.21	1233.41
Crystal system	Monoclinic	Triclinic	Triclinic	Triclinic
Space group	$P2_1/C$	$P\bar{1}$	$P\bar{1}$	$P\bar{1}$
a (Å)	20.596(2)	14.3519(8)	10.7026(14)	14.566(7)
b (Å)	18.1472(19)	14.5334(9)	14.5466(19)	18.193(9)
c (Å)	18.323(2)	14.7334(9)	17.401(2)	19.490(10)
α (°)	90	60.7330(10)	79.498(2)	104.437(8)
β (°)	115.313(2)	70.3360(10)	75.938(2)	101.602(8)
γ (°)	90	79.3630(10)	76.767(2)	109.253(8)
V (Å^3)	6190.8(11)	2523.7(3)	2535.0(6)	4489(4)
Z	4	2	2	2
D_{calc} (g/cm^3)	1.095	1.184	1.293	0.912
Radiation (λ), Å	Mo Kα (0.71073)	Mo Kα (0.71073)	Mo Kα (0.71073)	Mo Kα (0.71073)
$2\theta_{max}$ (°)	52.16	51.76	52.12	50.50
μ (cm^{-1})	9.85	12.72	20.64	7.34
$F(000)$	2210	960	1026	1308
Number of observed reflections	35477	9739	9806	15891
Number of parameters refined	12215	521	508	758
Goodness-of-fit	0.935	1.032	0.998	0.961
R_1	0.0922	0.0489	0.0581	0.1158
wR_2	0.2522	0.1323	0.1149	0.3723

Table 10
Summary of crystallographic data for **4a**, **4b** and **5**

	4a	**4b**	**5**
Formula	$C_{57}H_{61}N_2O_2P_2SiY$	$C_{57}H_{61}N_2O_2P_2SiLu$	$C_{29}H_{58}NO_3Si_2Y \cdot (C_7H_8)_{1/2}$
Molecular weight	985.02	1071.08	659.92
Crystal system	Triclinic	Triclinic	Monoclinic
Space group	$P\bar{1}$	$P\bar{1}$	$P2(1)/n$
a (Å)	13.7291(8)	13.6540(12)	15.3297(11)
b (Å)	20.0609(12)	20.1181(19)	14.1719(10)
c (Å)	20.9137(13)	20.8781(19)	18.4192(13)
α (°)	105.7750(10)	105.7280(10)	90.00
β (°)	105.2150(10)	105.0980(10)	103.5960(10)
γ (°)	93.2490(10)	93.2430(10)	90.00
V (Å^3)	5297.7(6)	5279.6(8)	3889.5(5)
Z	4	4	4
D_{calc} (g/cm^3)	1.235	1.347	1.127
Radiation (λ), Å	Mo Kα (0.71073)	Mo Kα (0.71073)	Mo Kα (0.71073)
$2\theta_{max}$ (°)	51.10	52.06	52.08
μ (cm^{-1})	12.25	19.95	15.89
$F(000)$	2064	2192	1420
Number of observed reflections	20364	20324	7660
Number of parameters refined	1073	1153	411
Goodness-of-fit	1.046	1.006	0.899
R_1	0.0704	0.0428	0.0463
wR_2	0.2120	0.1056	0.1059

5. Supplementary material

CCDC 607920, 607922, 622505, 607921, 619192, 619722 and 637044 contain the supplementary crystallographic data for **1**, **2a**, **2b**, **3**, **4a**, **4b** and **5**. These data can be obtained free of charge via http://www.ccdc.cam.ac.uk/conts/retrieving.html, or from the Cambridge Crystallographic Data Centre, 12 Union Road, Cambridge CB2 1EZ, UK; fax: (+44) 1223-336-033; or e-mail: deposit@ccdc.cam.ac.uk.

Acknowledgements

We thank financial supports from Jilin Provincial Science and Technology Bureau for Project No. 20050555; The National Natural Science Foundation of China for Project Nos. 20571072 and 20674081; The Ministry of Science and Technology of China for project No. 2005CB623802; "Hundred Talent Scientist Program" of CAS.

References

[1] (a) See reviews: Z. Hou, Y. Wakatsuki, Coord. Chem. Rev. 231 (2002) 1;
(b) J. Okuda, Dalton Trans. (2003) 2367;
(c) J. Gromada, J.F. Carpentier, A. Mortreux, Coord. Chem. Rev. 248 (2004) 397;
(d) J.Y. Hyeon, J. Gottfriendsen, F.T. Edelmann, Coord. Chem. Rev. 249 (2005) 2787;
(e) P.M. Zeimentz, S. Arndt, B.R. Elvidge, J. Okuda, Chem. Rev. 106 (2006) 2404 (and the references therein);
(f) Y.J. Luo, M. Nishiura, Z.M. Hou, J. Organomet. Chem. 692 (2007) 536.

[2] (a) Y. Zhang, Z. Hou, Y. Wakatsuki, Macromolecules 31 (1998) 8650;
(b) S. Kaita, Z. Hou, Y. Wakatsuki, Macromolecules 32 (1999) 9078;
(c) Z. Hou, Y. Zhang, H. Tezuka, P. Xie, O. Tardif, T.A. Koizumi, H. Yamazaki, Y. Wakatsuki, J. Am. Chem. Soc. 122 (2000) 10533;
(d) K.C. Hultzsch, P. Voth, K. Beckerle, T. Spaniol, J. Okuda, Organometallics 19 (2000) 228;
(e) Z. Hou, S. Kaita, Y. Wakatsuki, Macromolecules 34 (2001) 1539;
(f) Z. Hou, S. Kaita, Y. Wakatsuki, Pure Appl. Chem. 73 (2001) 291;
(g) Y. Luo, Y. Yao, Q. Shen, Macromolecules 35 (2002) 8670;
(h) Y. Luo, J. Baldamus, Z. Hou, J. Am. Chem. Soc. 126 (2004) 13910;
(i) E. Kirillov, C.W. Lehmann, A. Razavi, J.F. Carpentier, J. Am. Chem. Soc. 126 (2004) 12240;
(j) X. Li, Z. Hou, Macromolecules 38 (2005) 6767;
(k) X. Li, J. Baldamus, Z. Hou, Angew. Chem., Int. Ed.Engl. 44 (2005) 962;
(l) L. Zhang, Y. Luo, Z. Hou, J. Am. Chem. Soc. 127 (2005) 14562;
(m) O. Tardif, M. Nishiura, Z. Hou, Organometallics 22 (2003) 1171.

[3] (a) H. Yasuda, H. Yamamoto, K. Yokota, A. Nakamura, J. Am. Chem. Soc. 114 (1992) 4908;
(b) E. Ihara, M. Morimoto, H. Yasuda, Macromolecules 28 (1995) 7886;
(c) H. Yasuda, K. Yamamoto, W.E. Piers, D.J.H. Emslie, Coord. Chem. Rev. 233 (2002) 131;
(d) O.D. Cabaret, B.M. Vaca, D. Bourissou, Chem. Rev. 104 (2004) 6147;
(e) D. Cui, M. Nishiura, Z. Hou, Macromolecules 38 (2005) 4089;
(f) H. Yasuda, J. Organomet. Chem. 647 (2002) 128.

[4] (a) G. Jeske, E. Laurel, P. Schock, P.N. Swepston, H. Schumann, T.J. Marks, J. Am. Chem. Soc. 107 (1985) 8103;
(b) W. Roll, H-H. Brintzinger, B. Rieger, R. Zolk, Angew. Chem., Int. Ed. 29 (1990) 279;
(c) H. Schumann, J.A. Meese-Marktscheffel, L. Esser, Chem. Rev. 95 (1995) 865 (and references therein);
(d) S. Arndt, J. Okuda, Chem. Rev. 102 (2002) 1953 (and references therein);
(e) O. Tardif, M. Nishiura, Z. Hou, Tetrahedron 59 (2003) 10525.

[5] S. Bambirra, A. Meetsma, B. Hessen, J.H. Teuben, Organometallics 20 (2001) 782.

[6] (a) R. Duchateau, C.T. van Wee, A. Meetsma, J.H. Teuben, J. Am. Chem. Soc. 115 (1993) 4931;
(b) P.J. Bailey, S. Pace, Coord. Chem. Rev. 214 (2001) 91;
(c) G.R. Giesbrecht, G.D. Whitener, J. Arnold, Dalton Trans. 6 (2001) 923;
(d) Z. Lu, G.P.A. Yap, D.S. Richeson, Organometallics 20 (2001) 706.

[7] P.G. Hayes, W.E. Piers, L.W.M. Lee, L.K. Knight, M. Parvez, M.R.J. Elsegood, W. Clegg, Organometallics 20 (2001) 2533.

[8] (a) D.J.H. Emslie, W.E. Piers, R. McDonald, Dalton Trans. (2002) 293;
(b) D.J.H. Emslie, W.E. Piers, M. Parvez, R. McDonald, Organometallics 21 (2002) 4226.

[9] (a) Y.M. Yao, M.T. Ma, X.P. Xu, Y. Zhang, Q. Shen, W.T. Wong, Organometallics 24 (2005) 4014;
(b) X.P. Xu, M.T. Ma, Y.M. Yao, Y. Zhang, Q. Shen, Eur. J. Inorg. Chem. (2005) 676;
(c) P.N. O'Shaughnessy, P.D. Knight, C. Morton, K.M. Gillespie, P. Scott, Chem. Commun. (2003) 1770;
(d) D.V. Gribkov, K.C. Hultzsch, F. Hampell, Chem. Eur. J. 9 (2003) 4796;
(e) C.X. Cai, L. Toupet, C.W. Lehmann, J.F. Carpentier, J. Organomet. Chem. 683 (2003) 131;
(f) C.X. Cai, A. Amgoune, C.W. Lehmann, J.F. Carpentier, Chem. Commun. (2004) 330.

[10] I. Westmoreland, J. Arnold, Dalton Trans. (2006) 4155.

[11] H.W. Gorlitzer, M. Spiegler, R. Anwander, Dalton Trans. (1999) 4287.

[12] S. Bambirra, A. Meetsma, B. Hessen, A.P. Bruins, Organometallics 25 (2006) 3486.

[13] P.A. Cameron, V.C. Gibson, C. Redshaw, J.A. Segal, A.J.P. White, D.J. Williams, Dalton Trans. (2002) 415.

[14] H. Tsurugi, Y. Matsuo, T. Yamagata, K. Mashima, Organometallics 23 (2004) 2797.

[15] Y. Yang, S. Li, D. Cui, X. Chen, X. Jing, Organometallics 26 (2007) 671.

[16] P.D. Knight, A.J. Clarke, B.S. Kimberley, R.A. Jackson, P. Scott, Chem. Commun. (2002) 352.

[17] D.J.H. Emslie, W.E. Piers, M. Parvez, Dalton Trans. (2003) 2615.

[18] (a) D.P. Long, A. Chandrasekaran, R.O. Day, P.A. Bianconi, A.L. Rheingold, Inorg. Chem. 39 (2000) 4476;
(b) P.L. Arnold, S.A. Mungur, A.J. Blake, C. Wilson, Angew. Chem., Int. Ed. 42 (2003) 5981;
(c) M. E.G. Skinner, P. Mountford, Dalton Trans. (2002) 1694;
(d) J. Wang, X.D. Zhang, D.M. Fan, X. Ling, Chin. J. Inorg. Chem. 17 (2001) 755.

[19] During we were carrying out this work, complex **5** was reported by Bercaw et al. without crystallographic information and catalytic activity toward the polymerization of LA: S.C. Marinescu, T.A. Gapie, M.W. Day, J.E. Bercaw, Organometallics 26 (2007) 1178.

[20] A.R.F. Cox, V.C. Gibson, E.L. Marshall, A.J.P. White, D. Yeldon, Dalton Trans. (2006) 5014.

[21] (a) H. Ma, T.P. Spaniol, J. Okuda, Dalton Trans. (2003) 4770;
(b) O. Runte, T. Priermeier, R. Anwander, Chem. Commun. (1996) 1385.

[22] A. Amgoune, C.M. Thomas, T. Roisnel, J.F. Carpentier, Chem. Eur. J. 12 (2006) 169.

[23] F.M. Kerton, A.C. Whitewood, C.E. Willans, Dalton Trans. (2004) 2237.

[24] (a) C.G.J. Tazelaar, S. Bambirra, D. van Leusen, A. Meetsman, B. Hessen, J.H. Teuben, Organometallics 23 (2004) 936;
(b) S. Bambirra, S.J. Boot, D. van Leusen, A. Meetsman, B. Hessen, Organometallics 23 (2004) 1891;
(c) P.G. Hayes, G.C. Welch, D.J.H. Emslie, C.L. Noack, W.E. Piers, M. Parvez, Organometallics 22 (2003) 1577.

[25] The NMR spectrum for complex **5** in CD_2Cl_2 showed a different pattern from that in C_6D_6, especially the yttrium alkyl group, shifting up-field from $\delta = -0.45$ ppm to $\delta = -0.62$, indicating the change of geometry of the metal center. Resonances assigned to other groups are listed as follows: $\delta = -0.61$ (br, 4H, YCH_2SiMe_3), 0.40 (s, 18H, $YCH_2Si\mathit{Me}_3$), 1.40 (s, 9H, $C\mathit{Me}_3$), 1.57 (t, 2H, NCH_2CH_2OMe), 1.76 (s, 9H, $C\mathit{Me}_3$), 2.49 (m, 2H, $NCH_2\mathit{CH}_2OMe$), 2.49 (m, 2H, $N\mathit{CH}_2CH_2OMe$), 2.77 (t, 2H, NCH_2CH_2OMe), 3.10 (s, 6H, $O\mathit{Me}$), 3.44 (s, 2H, CH_2N), 6.88 (d, 1H, $J = 4$ Hz, Ar*H*), 7.53 (d, 1H, $J = 4$ Hz, Ar*H*).

[26] (a) X. Liu, X. Shang, T. Tang, N. Hu, F. Pei, D. Cui, X. Chen, X. Jing, Organometallics 26 (2007) 2747;
(b) H. Ma, J. Okuda, Macromolecules 38 (2005) 2665.

[27] M. Save, M. Schappacher, A. Soum, Macromol. Chem. Phys. 203 (2002) 889.

[28] B. Liu, D. Cui, J. Ma, X. Chen, X. Jing, Chem. Eur. J. 13 (2007) 834.

[29] X. Dai, A. Wong, S.C. Virgil, J. Org. Chem. 63 (1998) 2597.

[30] D. Simon, G.K. Julian, H.S. Tom, R.J.E. Mark, C. William, J. Organomet. Chem. 650 (2002) 231.